The Journal of Chemical Physics

# Effect of molecular size and hydrogen bonding on three surface-facilitated processes in molecular glasses: Surface diffusion, surface crystal growth, and formation of stable glasses by vapor deposition

Cite as: J. Chem. Phys. **150**, 024502 (2019); https://doi.org/10.1063/1.5079441
Submitted: 31 October 2018 . Accepted: 07 December 2018 . Published Online: 09 January 2019

Yinshan Chen, Zhenxuan Chen, Michael Tylinski, M. D. Ediger, and Lian Yu

The Journal of Chemical Physics ARTICLE scitation.org/journal/jcp

# Effect of molecular size and hydrogen bonding on three surface-facilitated processes in molecular glasses: Surface diffusion, surface crystal growth, and formation of stable glasses by vapor deposition

Cite as: J. Chem. Phys. 150, 024502 (2019); doi: 10.1063/1.5079441
Submitted: 31 October 2018 • Accepted: 7 December 2018 •
Published Online: 9 January 2019



Yinshan Chen,[1] Zhenxuan Chen,[1] Michael Tylinski,[2] M. D. Ediger,[2] and Lian Yu[1,2,a)]

## AFFILIATIONS

[1] School of Pharmacy, University of Wisconsin-Madison, Madison, Wisconsin 53705, USA
[2] Department of Chemistry, University of Wisconsin-Madison, Madison, Wisconsin 53706, USA

[a)] **Author to whom correspondence should be addressed:** lian.yu@wisc.edu

## ABSTRACT

Recent work has shown that diffusion and crystal growth can be much faster on the surface of molecular glasses than in the interior and that the enhancement effect varies with molecular size and intermolecular hydrogen bonds (HBs). In a related phenomenon, some molecules form highly stable glasses when vapor-deposited, while others (notably those forming extensive HBs) do not. Here we examine all available data on these phenomena for quantitative structure-property relations. For the systems that form no HBs, the surface diffusion coefficient $D_s$ decreases with increasing molecular size $d$ ($d = \Omega^{1/3}$, where $\Omega$ is the molecular volume); when evaluated at the glass transition temperature $T_g$, $D_s$ decreases ~5 orders of magnitude for 1 nm of increase in $d$. Assuming that center-of-mass diffusion is limited by the deepest part of the molecule in the surface-mobility gradient, these data indicate a mobility gradient in reasonable agreement with the Elastically Collective Nonlinear Langevin Equation theory prediction for polystyrene as disjointed Kuhn monomers. For systems of similar $d$, the $D_s$ value decreases with the extent of intermolecular HB, $x$ (HB), defined as the fraction of vaporization enthalpy due to HB. For both groups together (hydrogen-bonded and otherwise), the $D_s$ data collapse when plotted against $d/[1 - x(\mathrm{HB})]$; this argues that the HB effect on $D_s$ can be described as a narrowing of the surface mobility layer by a factor $[1 - x(\mathrm{HB})]$ relative to the van der Waals systems. Essentially the same picture holds for the surface crystal growth rate $u_s$. The kinetic stability of a vapor-deposited glass decreases with $x$(HB) but is not better organized by the combined variable $d/[1 - x(\mathrm{HB})]$. These results indicate that surface crystal growth depends strongly on surface diffusion, whereas the formation of stable glasses by vapor deposition may depend on other factors.



## INTRODUCTION

Glasses are amorphous solids produced by cooling liquids, condensing vapors, or evaporating solutions while preventing crystallization. Glasses combine crystal-like mechanical strength and liquid-like spatial uniformity, having many important applications in modern technologies. Being out-of-equilibrium materials, glasses are thermodynamically driven to crystallize and to age toward the equilibrium liquid state, both processes altering their physical properties. Thus a key issue in glass science is to understand and control physical stability.

Recent work has shown that the physical stability of molecular glasses is closely related to the molecular mobility at the free surface. Surface molecules can diffuse up to

8 orders of magnitude faster than bulk molecules when compared at the glass transition temperature $T_g$.[1–6] Surface mobility has been linked to two different aspects of glass stability. First, fast surface diffusion is responsible for fast surface crystal growth in many organic glasses.[7–10] For these systems, the surface crystal growth rate is nearly proportional to the surface diffusion coefficient.[6] A second consequence of surface mobility is the ability to prepare highly stable glasses by vapor deposition.[11] Deposition under suitable conditions can prepare glasses with extremely low energy, high density, and high resistance to thermal transformation; these properties would be expected for ordinary liquid-cooled glasses that have been aged for thousands of years. During deposition, surface molecules can utilize high mobility to find optimal packing before they are buried by the later-depositing molecules. Among other observations, the connection with surface mobility is supported by observations of increased stability at lower deposition rates.[12] Molecular systems with fast surface diffusion are generally able to form highly stable glasses by vapor deposition.[11,13,14]

While early work identified many systems that simultaneously exhibit high surface mobility, fast surface crystal growth, and ability to form stable glasses by vapor deposition, further studies of more diverse systems found that these surface-facilitated processes can depend strongly on molecular properties, in particular, molecular size and intermolecular hydrogen bonds (HBs). For molecules that do not form HBs [e.g., ortho-terphenyl (OTP), tris-naphthyl benzene (TNB), and polystyrene (PS) oligomers, see Scheme 1], surface diffusion systematically slows down by 5 orders of magnitude with increasing molecular size.[1,4,15] For molecules of similar sizes, increasing intermolecular HBs also reduces surface mobility. For example, OTP and sorbitol have similar sizes, but the surface diffusion of sorbitol is at least $10^5$ times slower at $T_g$.[16] In vapor deposition, molecules forming extensive intermolecular HBs (e.g., polyalcohols) have been observed to produce glasses of lower kinetic stability than non-hydrogen-bonding molecules at the same deposition rate[17] and require slower deposition in order to attain the same stability.[18]

Qualitative explanations have been proposed for the molecular dependence of surface mobility.[15,16] The size effect is attributed to a steep gradient of mobility beneath the free surface and the deeper penetration of a larger molecule into that gradient. This anchoring effect would lead to slower center-of-mass diffusion even though the top portion of the molecule is in a more mobile environment. The effect of HBs on surface diffusion is attributed to the robustness of HBs in surface layers, which makes the barrier for diffusion largely the same on the surface as in the bulk.[16] This too would lead to slower surface diffusion.

The goal of this work is to provide a quantitative test of the qualitative ideas described above using all available data in the literature. We show that for systems that form no HBs, the surface diffusion coefficient $D_s$ at $T_g$ decreases smoothly with increasing molecular size $d$ (defined as the cube root of the molecular volume), at a rate of ~5 orders of magnitude per nm. Assuming that the apparent $D_s$ reports the mobility of the deepest part of the molecule, the observed mobility gradient is in good agreement with the Elastically Collective Nonlinear Langevin Equation (ECNLE) theory prediction for polystyrene.[19] For systems of similar $d$, $D_s$ decreases with the extent of intermolecular HB, $x$(HB), defined as the fraction of vaporization enthalpy due to HB. For both groups together (hydrogen-bonded or otherwise), the $D_s$ data collapse when plotted against $d/[1 - x(\mathrm{HB})]$, suggesting that the HB effect on $D_s$ can be described as a narrowing of the surface mobility layer by a factor $[1 - x(\mathrm{HB})]$. These results support and give precision to the qualitative models proposed earlier. We also show that this two-parameter scheme involving $d$ and $x$(HB) can help understand surface crystal growth rates and the stability of vapor-deposited glasses.

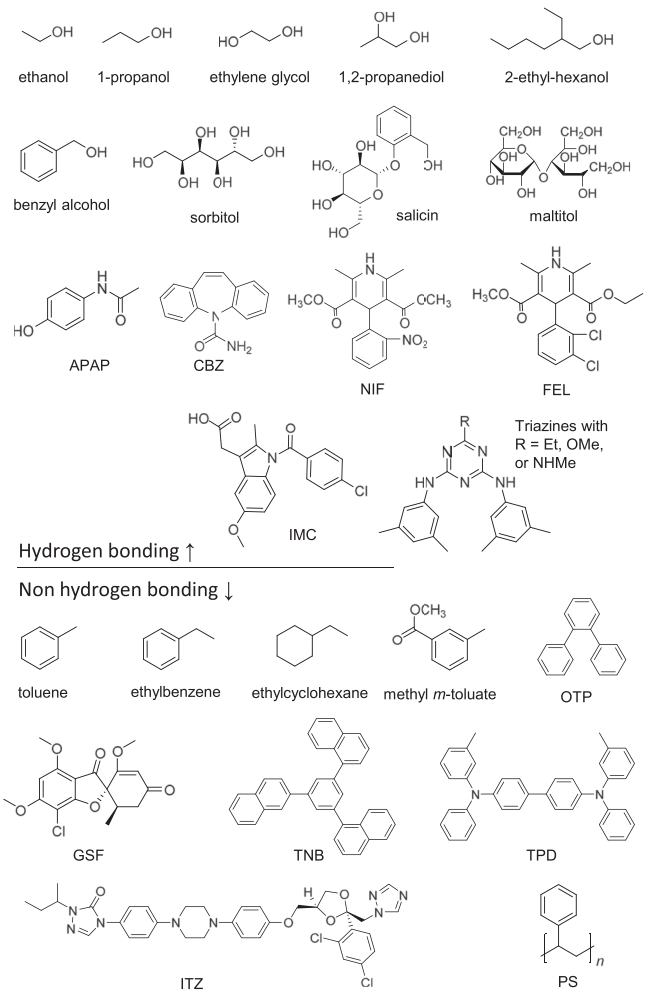


**SCHEME 1**. Structures of the molecules discussed in this work. They are separated into hydrogen bonding and non-hydrogen bonding. APAP: acetaminophen; CBZ: carbamazepine; NIF: nifedipine; FEL: felodipine; IMC: indomethacin; OTP: *ortho*-terphenyl; GSF: griseofulvin; TNB: *tris*-naphthyl benzene; TPD: *N*, *N*′-Bis(3-methylphenyl)-*N*, *N*′-diphenylbenzidine; ITZ: itraconazole; and PS: polystyrene.

## EXPERIMENTAL METHODS

In addition to literature data, surface crystal growth rates were measured for two additional systems, acetaminophen (APAP) and itraconazole (ITZ), to extend the available data to higher hydrogen bonding extent and larger molecular size. APAP (purity ≥ 99%) was purchased from Sigma-Aldrich, and ITZ (purity ≥ 98%) was purchased from Alfa Aesar. To prepare a sample for surface crystal growth measurement, ~5 mg of the crystalline substance was melted on a clean square coverslip at 5 K above its melting point and covered with a smaller round coverslip (typically 15 mm in diameter). The assembly was cooled to below $T_g$ by contact with a metal block pre-equilibrated at room temperature. The square coverslip was detached by bending its edges away from the organic glass, creating a glass film 10–100 $\mu$m thick with a free surface. Surface crystallization was initiated by seeding with the as-received crystalline material. The rate of crystal growth was measured through a light microscope (Olympus BX3-URA) at a constant temperature maintained by a Linkam stage (THMS 600E) or a custom-built mini-oven. The samples were purged with dry $N_2$ during measurement. To prepare a sample for crystal growth measurement in the bulk, the same sample preparation procedure was applied except that the top coverslip was not removed. Crystal growth in the bulk was initiated by seeding on the exposed edge of the sample between coverslips. Polymorphs were identified by X-ray powder diffraction (Bruker D8 Advance).

## RESULTS AND DISCUSSION

### Extent of intermolecular HB from vaporization enthalpies

To measure the extent of intermolecular HBs in a liquid, we introduce the following quantity:

**TABLE I**. Extents of hydrogen bonding in molecular liquids calculated with a replacement method.

| | $H_{vap}$ (kJ/mol) | $H_{vap}$ (kJ/mol), homomorph | x(HB) |
|---|---|---|---|
| Ethanol | 41.7 | 17.0 (propane) | 0.59 |
| 1-propanol | 46.4 | 21.7 (butane) | 0.53 |
| Ethylene glycol | 68.2 | 21.7 (butane) | 0.68 |
| 1,2-propanediol | 58.8 | 26.4 (isopentane) | 0.55 |
| Benzyl alcohol | 65.1 | 40.5 (ethylbenzene) | 0.38 |
| 2-ethyl-hexanol | 69.8 | 45.2 (3-ethyl-heptane) | 0.35 |
| APAP | 118 | 64.0 | 0.46 |
| CBZ | 103 | 94.1 | 0.089 |
| NIF | 134 | 125 | 0.065 |
| FEL | 135 | 129 | 0.043 |
| Triazine Et | 139 | 125 | 0.10 |
| Triazine OMe | 140 | 126 | 0.10 |
| Triazine NHMe | 147 | 125 | 0.15 |
| IMC | 159 | 136 | 0.14 |
| Sorbitol | 157 | 59.2 | 0.62 |
| Salicin | 183 | 95.6 | 0.48 |
| Maltitol | 262 | 109 | 0.58 |

$$x(\mathrm{HB}) = \Delta H_{vap}(\mathrm{HB})/\Delta H_{vap}, \quad (1)$$

where $\Delta H_{vap}$ is the vaporization enthalpy and $\Delta H_{vap}$(HB) is the portion of $\Delta H_{vap}$ attributed to HBs. Following Bondi,[20] $\Delta H_{vap}$(HB) is calculated by a "replacement method,"

$$\Delta H_{vap}(\mathrm{HB}) = \Delta H_{vap} - \Delta H_{vap}{}^{*}, \quad (2)$$

where $\Delta H_{vap}{}^{*}$ is the $\Delta H_{vap}$ of a "homomorph" in which the HB functional group is replaced by a non-hydrogen bonding group. For an alcohol, for example, the hydroxyl group OH is replaced by the methyl group $CH_3$, on the basis that the two functional groups make similar contributions to the dispersion energy. It was found that the increment $\Delta H_{vap}$(HB) is nearly constant for monoalcohols of different carbon numbers,

**TABLE II**. Surface diffusion coefficients $D_s$ of molecular glasses along with their molecular weights, extents of hydrogen bonding, densities, and molecular sizes.

| | M (g/mol) | $T_g$ (K) | $\rho$ at $T_g$ (g/cm$^3$) | $\rho$ (References) | $d$ (nm) | x(HB) | log $D_s$ at $T_g$ (m$^2$/s) | $D_s$ (References) |
|---|---|---|---|---|---|---|---|---|
| OTP | 230.3 | 246 | 1.12 | 28 | 0.70 | 0 | −11.9 | 1 |
| GSF | 352.8 | 361 | 1.35 | 29 | 0.76 | 0 | −12.4 | 6 |
| TNB | 456.6 | 347 | 1.15 | 30 | 0.87 | 0 | −13.3 | 4 |
| TPD | 516.7 | 330 | 1.19 | 5 | 0.90 | 0 | −14.2 | 5 |
| PS1100 | 990 | 307 | 1.03 | 31 | 1.17 | 0 | −15.3 | 15 |
| PS1700 | 1600 | 319 | 1.03 | 31 | 1.37 | 0 | −16.0 | 15 |
| PS2400 | 2264 | 337 | 1.03 | 31 | 1.54 | 0 | −16.0 | 32 |
| PS3000 | 2752 | 343 | 1.03 | 31 | 1.64 | 0 | −16.3 | 33 |
| NIF | 346.3 | 315 | 1.36 | 34 | 0.75 | 0.065 | −13.7 | 3 |
| IMC | 357.8 | 315 | 1.34 | 35 | 0.76 | 0.14 | −14.0 | 2 |
| Triazine Et | 347.5 | 314 | 1.07[a] | ... | 0.81 | 0.10 | −14.4 | 36 |
| Triazine OMe | 349.4 | 330 | 1.07[a] | 23 | 0.82 | 0.10 | −14.0 | 36 |
| Triazine NHMe | 348.5 | 360 | 1.07[a] | ... | 0.81 | 0.15 | −15.6 (ub)[b] | 36 |
| Sorbitol | 182.2 | 269 | 1.47 | 37 | 0.59 | 0.62 | −16.4 (ub)[b] | 16 |
| Maltitol | 344.3 | 317 | 1.51 | 37 | 0.72 | 0.58 | −16.4 (ub)[b] | 16 |

[a]Estimated as 95% of crystal density. Triazine OMe crystal density is from Ref. 23; the same value is assumed for triazine Et and NHMe.
[b]ub: upper bound.

indicating that each OH makes a similar contribution to $\Delta H_{vap}$.[20] For non-hydroxyl groups, we use the following replacement scheme: –COOH (carboxylic acid) by $-CO-CH_3$ (ketone), $-NH_2$ (primary amine) by $-CH_3$, –NH– (secondary amine) by $-CH_2-$, $-CO-NH_2$ (primary amide) by $-CO-CH_3$ (ketone), and –CO–NH– (secondary amide) by $-CO-CH_2-$.

Some $\Delta H_{vap}$ values necessary for computing $x$(HB) are reported[21] but not all. For consistency, we use the group additivity method of Chickos *et al.* to calculate all $\Delta H_{vap}$ values.[22] Chickos *et al.* calibrated their method on a total of 147 experimental $\Delta H_{vap}$ values, reproducing the values within 5% (comparable to the measurement error). For each liquid of this study, the method calculates $\Delta H_{vap}$ at 298 K in units of kcal/mol as follows:

$$\Delta H_{vap} = 1.12 n_c + 0.71 + \sum F_i b_i + C, \quad (3)$$

where $n_c$ is the number of carbon atoms in the molecule and the numbers 1.12 and 0.71 both carry the unit kcal/mol. The term $F_i b_i$ is the contribution of a given functional group $i$ to the total $\Delta H_{vap}$, with $b_i$ being its characteristic enthalpy increment and $F_i$ being a weighting factor dependent on its location in the molecule. For example, for an OH group in an alcohol, $b$ = 7.02 kcal/mol and $F$ = 1.62 for the OH in 1-propanol and 0.60 for the OH in 2-propanol. The $C$ term in Eq. (3) contains corrections for the branching of a carbon chain, intramolecular hydrogen bonding, and other effects.

Table I shows the results of this calculation for the systems discussed in this work ($n_c$, $\Sigma F_i b_i$, and $C$ are listed in Table S1 in supplementary material). For non-HB systems (excluded from Table I), $x$(HB) = 0, whereas the polyalcohol sorbitol has a high $x$(HB) of 0.62. In the three triazine molecules studied here (Et, OMe, and NHMe, see Scheme 1), the NH group of one molecule is hydrogen-bonded to a triazine nitrogen of another.[23] At present, the method of Chickos *et al.* provides no $b$ values for this type of HB. We have estimated this $b$ value to be 7 kJ/mol from the difference in $\Delta H_{vap}$ between 2-methylaminopyridine and ethyl benzene.[21] In addition, we assume that each tertiary ring nitrogen in CBZ and IMC makes the same contribution to $\Delta H_{vap}$ as a CH group at the same location.

### Effects of molecular size and intermolecular HB on surface diffusion, surface crystal growth, and stability of vapor-deposited glasses

Table II shows the surface diffusion coefficients $D_s$ of molecular glasses along with other relevant properties. The molecular size $d$ is calculated from $d = \Omega^{1/3} = [M/(\rho N_A)]^{1/3}$, where $\Omega$ is the molecular volume, $M$ is the molecular weight, $\rho$ is the density at $T_g$, and $N_A$ is the Avogadro's constant. For comparison of different systems, the $D_s$ values are given at $T_g$ where different molecular glasses have similar bulk mobility. Note that the $D_s$ values at $T_g$ span approximately 5 orders of magnitude. This contrasts with the smaller range for the bulk diffusion coefficients $D_v$ at $T_g$; for the available data (OTP, TNB, IMC, and 1.9 kg/mol PS),[24–27] the average $D_v$ at $T_g$ is $10^{-20}$ $m^2/s$ with a standard deviation of 0.6 decade.

In Fig. 1(a), the $D_s$ value at $T_g$ is plotted against $d$. As a single group, the $D_s$ values show no strong correlation with $d$, but a clear correlation is seen for the non-hydrogen-bonding group ($x$(HB) = 0). For this group, $D_s$ smoothly decreases with

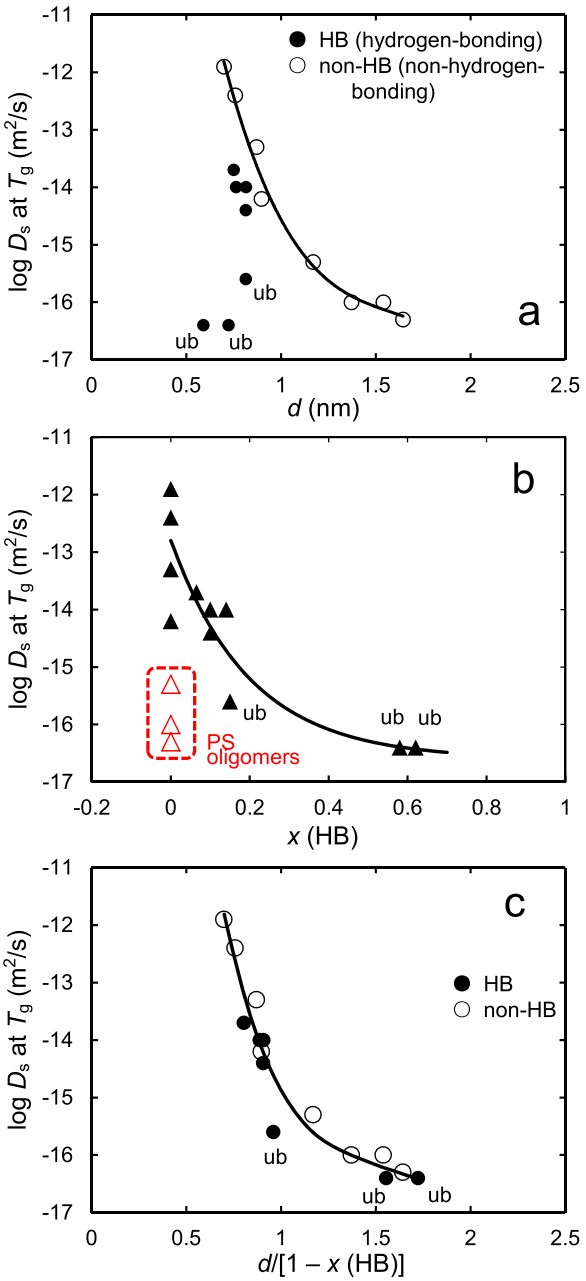


**FIG. 1.** Surface diffusion coefficient $D_s$ at $T_g$ plotted as a function of (a) $d$, (b) $x$(HB), and (c) $d/[1 - x(HB)]$. "ub" stands for "upper bound" (see Table II). The curves are guide to the eye.

increasing $d$, insensitive to the details of the molecular structures (Scheme 1). This indicates that molecular size has a controlling effect on surface diffusion in the absence of HBs; we will discuss this result shortly. For the HB group, $D_s$ is substantially smaller than that for the non-HB group at the same $d$, indicating that hydrogen bonding is an independent factor controlling $D_s$. For some systems in this figure, surface diffusion was too slow to be measured using the surface-grating method and only upper bounds have been reported for $D_s$.[16,36] These are indicated as "ub" in Fig. 1. The actual $D_s$ values are expected to be smaller than these upper bounds but larger than the bulk diffusivity $D_v$.

In Fig. 1(b), the $D_s$ value at $T_g$ is plotted against $x$(HB). If we consider the smaller molecules (solid symbols) separately from the PS oligomers (open symbols), we see a broad trend of $D_s$ decreasing with increasing $x$(HB). There is a wide scatter of data points at $x$(HB) = 0, reflecting the molecular size effect on $D_s$ for the non-HB group (OTP, GSF, TNB, and TPD). The PS oligomers are outliers to the trend for the small molecules, again indicating an independent effect of molecular size on surface diffusion.

Although neither $d$ nor $x$(HB) alone can organize all the data, we find that all the data collapse to a common trend when plotted against the combined variable $d/[1 - x(\mathrm{HB})]$. This is seen in Fig. 1(c). This result suggests that the effect of HBs can be understood as a modification of the surface-mobility gradient in a van der Waals system, as we discuss below.

For van der Waals glass-formers (no HBs), we attribute the dependence of $D_s$ on molecular size $d$ [Fig. 1(a), open symbols] to the presence of a steep mobility gradient beneath the free surface and to the deeper penetration of a larger molecule into that gradient.[15] Building on this idea, we make a quantitative estimate of the mobility gradient from the available $D_s$ data. The mobility gradient can be expressed as a local relaxation time as a function of depth $z$, $\tau_\alpha(z)$. Assuming that the deepest, least-mobile part of the molecule determines its center-of-mass diffusion, we can write $D_s = d^2/[4\tau_\alpha(z = d)]$, where $d$ is the molecular diameter. This yields an equation for estimating $\tau_\alpha$ at the depth $z = d$, namely, $\tau_\alpha(z = d) = d^2/(4D_s)$. Figure 2 (solid symbols) shows the result of this calculation using all available $D_s$ data on van der Waals glass-formers evaluated at $T_g$. To be specific, we use the $T_g$ onset during heating detected by DSC at 10 K/min after cooling at 10 K/min; at this $T_g$, the bulk relaxation time $\tau_\alpha$ is approximately 10 s. Figure 2 shows that $\tau_\alpha$ increases smoothly with depth $z$, tending toward the bulk value $\tau_\alpha \approx 10$ s. This smooth increase in $\tau_\alpha$ with $z$,

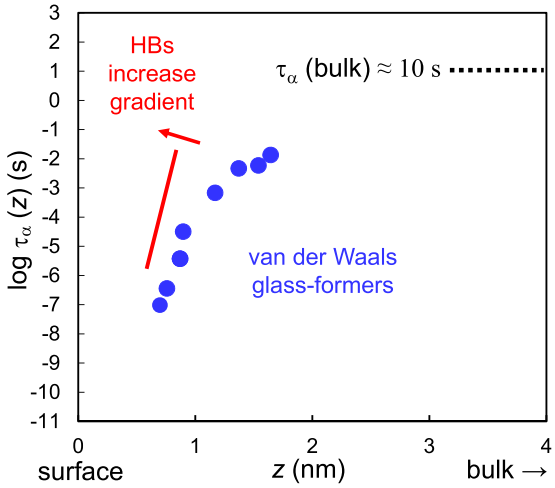


**FIG. 2.** Surface-mobility gradients in molecular glasses at $T_g$. The solid circles are the local relaxation times calculated from the surface diffusion coefficients of van der Waals glass-formers (e.g., OTP and TNB) assuming that the deepest, least-mobile part of the molecule determines its center-of-mass diffusion. The effect of HBs is to increase the slope of the gradient by a factor of $1/[1 - x(\mathrm{HB})]$.

**TABLE III.** Surface crystal growth rates $u_s$ of molecular glasses along with their molecular weights, extents of hydrogen bonding, densities, and calculated molecular sizes.

| | M (g/mol) | $T_g$ (K) | $\rho$ at $T_g$ (g/cm$^3$) | $\rho$ (References) | $d$ (nm) | $x$ (HB) | log $u_s$ at $T_g$ (m/s)[a] | $u_s$ (References) |
|---|---|---|---|---|---|---|---|---|
| OTP | 230.3 | 246 | 1.12 | 28 | 0.70 | 0 | −6.8 | 41 |
| GSF | 352.8 | 361 | 1.35 | 29 | 0.76 | 0 | −7.6 (I) | 8 |
| TNB | 456.6 | 347 | 1.15 | 30 | 0.87 | 0 | −8.5 | 4 |
| ITZ | 705.6 | 328 | 1.27 | 42 | 0.97 | 0 | −9.6 (I) | This work |
| APAP | 151.2 | 294 | 1.22 | 43 | 0.59 | 0.46 | −8.1 (I) | 44, this work |
| CBZ | 236.3 | 319 | 1.14 | 45 | 0.70 | 0.089 | −8.2 (IV)[b] | 45, at $T_g$ − 6K |
| NIF | 346.3 | 315 | 1.36 | 34 | 0.75 | 0.065 | −8.2 (β) | 9 |
| FEL | 384.3 | 316.5 | 1.33 | 46 | 0.78 | 0.043 | −8.0 (I) | 47 |
| IMC | 357.8 | 315 | 1.34 | 35 | 0.76 | 0.14 | −8.8 (α and γ) | 10 |
| Salicin | 286.3 | 332 | 1.34[c] | 48 | 0.71 | 0.48 | −10.0 | 44 |
| Maltitol | 344.3 | 317 | 1.51 | 37 | 0.72 | 0.58 | −12.4 (ub)[d] | 16 |

[a]Symbols in parentheses indicate the polymorphs.
[b]For CBZ, the fastest $u_s$ is provided (polymorph IV); for other polymorphs, log $u_s$ (m/s) = −8.8 (I), −8.7(III).[45]
[c]$\rho$ of the glass is estimated as 95% of the crystal density.
[d]ub: upper bound.

regardless of the exact molecular structure, argues that the van der Waals glass-formers have a *similar* surface mobility gradient when compared at $T_g$. The initial loss of mobility with depth is quite steep and quasi-exponential, roughly given by $d \log \tau_\alpha / dz \approx 7/\text{nm}$. This mobility gradient agrees reasonably well with that predicted by the Elastically Collective Nonlinear Langevin Equation (ECNLE).[19] According to this theory, a surface molecule is more mobile than a bulk molecule because it has fewer neighbors and lower elastic penalty for rearrangement. ECNLE predicts approximately the same gradient as shown in Fig. 2 for a polystyrene (PS) melt near $T_g$ without chain connectivity (disjointed Kuhn spheres).[19] Within this theory, the prediction for PS is expected to represent a wide class of van der Waals glass-formers like OTP and TNB.[19] This agreement between the experiment and theory provides support for our interpretation of the molecular-size effect on surface diffusion.

In Fig. 2, we indicate how introducing HBs might modify the mobility gradient in a van der Waals system. We suggest that HBs increase the steepness of the gradient or equivalently reduce its thickness. Simulations have shown that in water, surface and bulk molecules have similar diffusion rates,[38] likely a consequence of the preservation of HBs (each molecule has 3.2 HBs on the surface vs. 3.8 in the bulk).[38] This is in sharp contrast to a Lennard-Jones liquid in which a surface particle has about half as many nearest neighbors compared to a bulk particle and as a result faster lateral diffusion.[39,40] We imagine a similar situation for hydrogen-bonded molecular glasses: each surface molecule has nearly the same number of HBs as a bulk molecule and therefore has lower mobility when compared to a surface particle in a van der Waals system. In Fig. 2, we illustrate the effect of HBs using a tilted line relative to the points for the van der Waals systems; introducing HBs would increase the steepness of the mobility gradient and reduce its thickness. The fact that the $D_s$ data collapse on the combined variable $d/[1 - x(\text{HB})]$ suggests that HBs reduce the thickness of the mobile layer by a factor of $[1 - x(\text{HB})]$. This is a sensible result since $[1 - x(\text{HB})]$ is the fraction of molecular interactions that are van der Waals in nature and might serve as a measure of how closely a system still resembles a pure van der Waals system when HBs are present.

We now extend the analysis of the effect of molecular size and HBs to the rate of surface crystal growth $u_s$. Table III shows the $u_s$ values of molecular glasses along with other information. The $u_s$ measurements of APAP and ITZ are described in the supplementary material. We find that essentially the same picture holds as in the case of surface diffusion.

In Fig. 3(a), $u_s$ at $T_g$ is plotted as a function of $d$. A similar situation is seen here as in Fig. 1(a). As a single group, the $u_s$ values show no correlation with $d$, but a correlation is seen for the non-HB group (open symbols), with $u_s$ decreasing with increasing $d$. For the HB group, $u_s$ is substantially smaller relative to the non-HB group when compared at a similar $d$. In Fig. 3(b), $u_s$ at $T_g$ is plotted against $x$(HB). There is considerable scattering, while a broad decreasing trend can be noticed.

In Fig. 3(c), we plot $u_s$ as a function of the combined variable $d/[1 - x(\text{HB})]$. In this format, we see significantly improved collapse of data onto a common trend. The collapse is not perfect, but it is encouraging that the same combined variable can organize both $D_s$ and $u_s$ data. This is consistent with the report of Huang *et al.*[6] who observed a power-law relation for many molecular glasses, $u_s \propto D_s^{0.9}$, with the

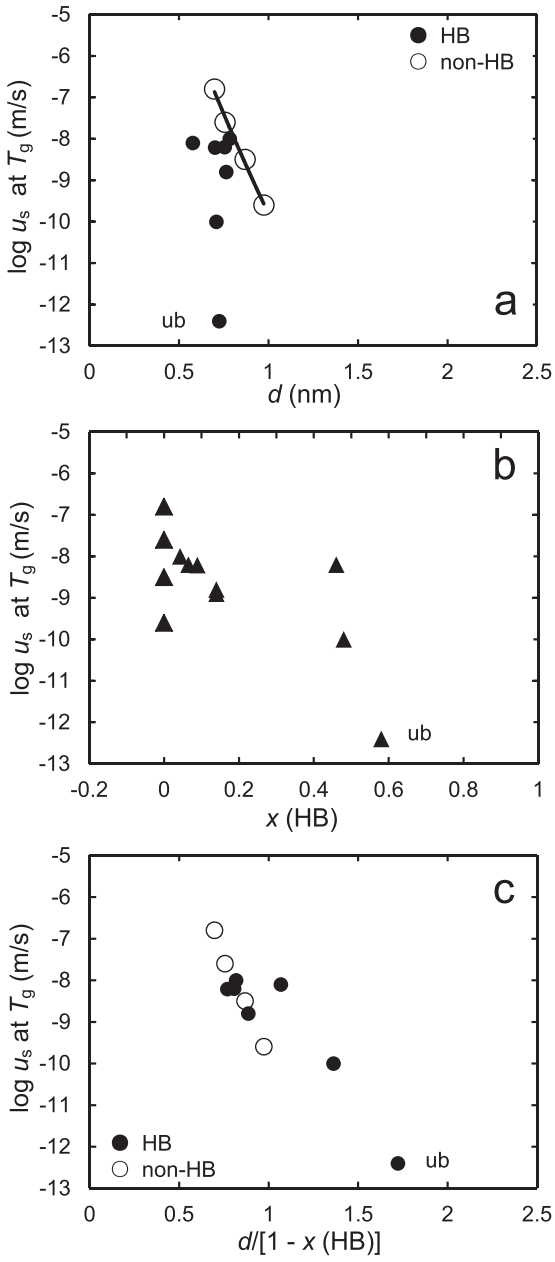


**FIG. 3**. Surface crystal growth rate $u_s$ at $T_g$ plotted as a function of (a) $d$, (b) $x$(HB), and (c) $d/[1 - x(\text{HB})]$. "ub" stands for "upper bound." The line is guide to the eye.

$u_s$ values clustering within one decade of each other at a common $D_s$.

Finally, we analyze the effect of molecular size and HBs on the formation of stable glasses by vapor deposition. Table IV shows the kinetic stability of molecular glasses prepared by vapor deposition and other physical properties. These glasses were deposited under similar conditions: the deposition rate was ~0.2 nm/s, and the substrate temperature was chosen to maximize stability (0.84–0.92 $T_g$). These are the conditions that yielded the most stable glasses for molecules that form no or limited HBs. The kinetic stability corresponds to the time for the glass to transform into a supercooled liquid scaled by the α relaxation time of the liquid, $t_{transformation}/\tau_\alpha$. For an ordinary, liquid-cooled glass, this ratio is approximately unity. The deposited films tested had similar thicknesses except for the triazine glasses. The triazine data were acquired under somewhat different conditions that could shift the observed transformation time by up to 0.3 decades; we have not made this adjustment as this would have a negligible impact on our analysis of the data. In Table IV, note the large range of kinetic stability (spanning more than 4 orders of magnitude) for the glasses of different molecules produced under similar conditions of vapor deposition.

In Fig. 4(a), the kinetic stability of vapor-deposited glasses is plotted as a function of $d$. There is no clear correlation other than the fact that the non-HB group is above (more stable) than the HB group. Figure 4(b) plots the kinetic stability against $x$(HB). A clear correlation is seen with the kinetic stability decreasing as the extent of HBs increases. This confirms the conclusion of Tylinski *et al.*[17] in a quantitative format. In Fig. 4(c), the kinetic stability of a vapor-deposited glass is plotted against the combined variable $d/[1 - x(\text{HB})]$. There is a decreasing trend, consistent with the control of surface mobility over the formation of stable glasses; however, the quality of data collapse is not significantly improved over Fig. 4(b). Overall, the kinetic stability of vapor-deposited glasses shows a similar response to $x$(HB) as $D_s$ and $u_s$, but its response to $d$ is obviously different. The ability to form stable glasses by vapor deposition should also depend on additional factors, such as the existence of a low-energy target structure to which freshly deposited molecules are driven to evolve. It is possible that the surface relaxation process responsible for stable-glass formation does not have a simple relationship with translational surface diffusion. While translation across many molecular diameters occurs during surface crystal growth and is required for surface diffusion to be detected, stable glass formation depends on improvements in local packing that in principle could be accomplished with very little translational motion. Even for bulk glass formers, translational diffusion coefficients are partially decoupled from structural relaxation times, indicating the complex relationship between these quantities.[24–26] Another complicating factor is that the kinetic stability was assessed at a higher temperature than the formation of the glass. The kinetic barrier for the transformation process may be different from that for the stable glass formation process. It may be of interest to learn whether a different measure of vapor-deposited glass stability measured at the formation temperature (e.g., density and enthalpy) has a similar dependence on $d$ and $x$(HB) as surface diffusion and surface crystal growth.

**TABLE IV**. Kinetic stability of vapor-deposited molecular glasses along with their molecular weights, extents of hydrogen bonding, densities, and calculated molecular sizes.

| | M (g/mol) | $T_g$ (K) | $\rho$ at $T_g$ (g/cm$^3$) | $\rho$ (References) | $d$ (nm) | $x$ (HB) | log ($t_{transformation}/\tau_\alpha$) | References |
|---|---|---|---|---|---|---|---|---|
| Toluene | 92.1 | 117 | 1.02[a] | 49 | 0.53 | 0 | 3.4 | 17 |
| Ethylbenzene | 106.2 | 115 | 1.02[a] | 49 | 0.56 | 0 | 3.1 | 17 |
| Ethylcyclohexane | 114.4 | 104.5 | 0.94[b] | 49 and 50 | 0.58 | 0 | 4.0 | 17 |
| Methyl *m*-toluate | 150.2 | 169 | 1.17[c] | 50 and 51 | 0.60 | 0 | 3.3 | 17 |
| OTP | 230.3 | 246 | 1.12 | 28 | 0.70 | 0 | 4.9 | 17 |
| TNB | 456.6 | 347 | 1.15 | 30 | 0.87 | 0 | 4.0 | 17 |
| TPD | 516.7 | 330 | 1.19 | 5 | 0.90 | 0 | 4.4 | 17 |
| Triazine Et | 347.5 | 314 | 1.07[d] | ... | 0.81 | 0.10 | 3.3 | 52 |
| Triazine OMe | 349.4 | 330 | 1.07[d] | 23 | 0.82 | 0.10 | 3.2 | 52 |
| Triazine NHMe | 348.4 | 360 | 1.07[d] | ... | 0.81 | 0.15 | 1.9 | 52 |
| IMC | 357.8 | 315 | 1.34 | 35 | 0.76 | 0.14 | 3.7 | 17 |
| Ethanol | 46.9 | 97 | 0.94[a] | 49 | 0.43 | 0.59 | 1.4 | 17 |
| 1-propanol | 61.2 | 99 | 0.95[a] | 49 | 0.47 | 0.53 | 0.3 | 17 |
| Ethylene glycol | 62.1 | 150 | 1.20[a] | 49 | 0.44 | 0.68 | 0.7 | 17 |
| 1,2-propanediol | 77.3 | 168 | 1.13 | 53 | 0.48 | 0.55 | 0.7 | 17 |
| Benzyl alcohol | 109.6 | 168 | 1.11[d] | 54 | 0.54 | 0.38 | 3.4 | 17 |
| 2-ethyl-hexanol | 132.7 | 143 | 0.94 | 55 | 0.61 | 0.35 | 2.0 | 17 |

[a]Estimated by extrapolating liquid density to $T_g$.
[b]Estimated by extrapolating ethylcyclohexane density at 293 K to $T_g$ assuming that its temperature dependence is the same as that for cyclohexane.
[c]Estimated by extrapolating methyl *m*-toluate density at 293 K to $T_g$ assuming that its temperature dependence is the same as that for methyl benzoate.
[d]Estimated as 95% of crystal density. Triazine OMe crystal density is from Ref. 23; the same value is assumed for triazine Et and NHMe.

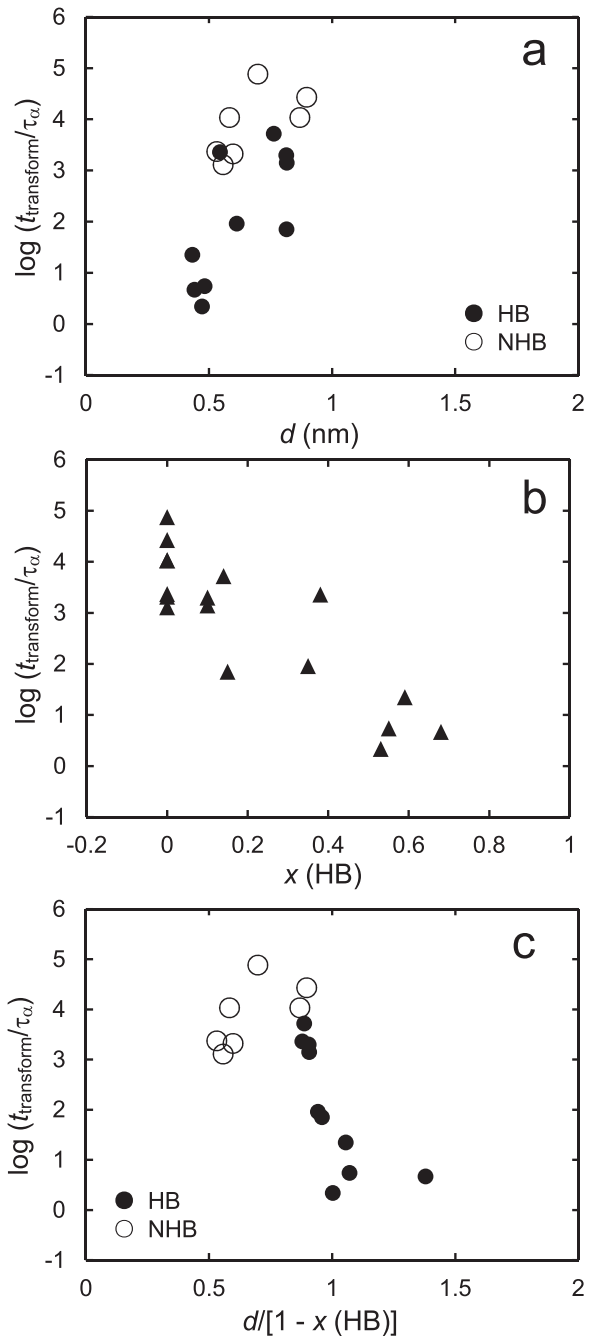


**FIG. 4**. Kinetic stability of a vapor-deposited glass as a function of (a) $d$, (b) $x$(HB) and (c) $d/[1 - x(\mathrm{HB})]$.

## CONCLUSION

We have examined how the molecular size and the extent of hydrogen bonding influence three processes in molecular glasses that involve surface mobility: surface diffusion, surface crystal growth, and the formation of stable glasses by vapor deposition. For systems that form no HBs, the surface diffusion coefficient $D_s$ at $T_g$ decreases with increasing molecular size $d$, at a rate of ~5 orders of magnitude per nanometer. Assuming that center-of-mass diffusion is limited by the deepest, least-mobile part of the molecule in the surface-mobility gradient, the available data indicate a mobility gradient in reasonable agreement with the ECNLE prediction. For systems of similar $d$, $D_s$ decreases with the extent of intermolecular HB, $x$(HB). It is remarkable that for all the systems studied (hydrogen-bonded or not), the $D_s$ data collapse when plotted against $d/[1 - x(\mathrm{HB})]$; this argues that the HB effect on $D_s$ can be described as a narrowing of the surface mobility layer by a factor $[1 - x(\mathrm{HB})]$. Essentially the same picture holds for the surface crystal growth rate $u_s$. The kinetic stability of a vapor-deposited glass decreases with $x$(HB) and marginally organized by the combined variable $d/[1 - x(\mathrm{HB})]$. These results indicate that surface crystal growth is controlled by surface diffusion, whereas the formation of stable glasses by vapor deposition may depend on other factors.

Molecular mobility is expected to decrease sharply from the free surface to the interior of a glass. At present, the information is quite limited about the dimension and the steepness of this gradient. The available surface diffusion data on van der Waals glass-formers (e.g., OTP, TNB, and PS oligomers) suggest that these systems have a similar surface-mobility gradient when compared at $T_g$. This picture might come as a surprise given that these systems contain molecules of different sizes and mobility might be expected to decrease by the same amount for every molecular diameter of increase in depth, not every nanometer. This picture could be tested by simulations. This work has also found that the slower surface diffusion in hydrogen-bonded systems can be described as a narrowing of the surface mobile layer relative to van der Waals systems. Simulations can also help evaluate this conclusion.

## SUPPLEMENTARY MATERIAL

See supplementary material for calculation of vaporization enthalpies and for surface crystal growth measurements of APAP and ITZ.

## ACKNOWLEDGMENTS

Y.C., Z.C., and L.Y. thank the Bill and Melinda Gates Foundation and the NSF supported UW – Madison MRSEC (Grant No. DMR-1720415) for supporting this work. M.D.E. and M.T. acknowledge NSF (Grant No. CHE-1564663) for support.

## REFERENCES

[1]W. Zhang, C. W. Brian, and L. Yu, J. Phys. Chem. B **119**, 5071 (2015).
[2]L. Zhu, C. W. Brian, S. F. Swallen, P. T. Straus, M. D. Ediger, and L. Yu, Phys. Rev. Lett. **106**, 256103 (2011).
[3]C. W. Brian and L. Yu, J. Phys. Chem. A **117**, 13303 (2013).
[4]S. Ruan, W. Zhang, Y. Sun, M. D. Ediger, and L. Yu, J. Chem. Phys. **145**, 064503 (2016).
[5]Y. Zhang and Z. Fakhraai, Soft Matter **12**, 9115 (2016).

[6]C. Huang, S. Ruan, T. Cai, and L. Yu, J. Phys. Chem. B **121**, 9463 (2017).
[7]Y. Sun, L. Zhu, K. L. Kearns, M. D. Ediger, and L. Yu, Proc. Natl. Acad. Sci. U. S. A. **108**, 5990 (2011).
[8]Q. Shi and T. Cai, Cryst. Growth Des. **16**, 3279 (2016).
[9]L. Zhu, L. Wong, and L. Yu, Mol. Pharm. **5**, 921 (2008).
[10]M. Hasebe, D. Musumeci, T. C. Powell, T. Cai, E. Gunn, L. Zhu, and L. Yu, J. Phys. Chem. B **118**, 7638 (2014).
[11]S. F. Swallen, K. L Kearns, M. K. Mapes, Y. S. Kim, R. J. McMahon, M. D. Ediger, T. Wu, L. Yu, and S. Satija, Science **315**, 353 (2007).
[12]K. L. Kearns, S. F. Swallen, M. D. Ediger, T. Wu, Y. Sun, and L. Yu, J. Phys. Chem. B **112**, 4934–4942 (2008).
[13]L. Zhu and L. Yu, Chem. Phys. Lett. **499**, 62 (2010).
[14]K. R. Whitaker, M. Tylinski, M. Ahrenberg, C. Schick, and M. D. Ediger, J. Chem. Phys. **143**, 084511 (2015).
[15]W. Zhang and L. Yu, Macromolecules **49**, 731 (2016).
[16]Y. Chen, W. Zhang, and L. Yu, J. Phys. Chem. B **120**, 8007 (2016).
[17]M. Tylinski, Y. Z. Chua, M. S. Beasley, C. Schick, and M. D. Ediger, J. Chem. Phys. **145**, 174506 (2016).
[18]M. Tylinski, M. S. Beasley, Y. Z. Chua, C. Schick, and M. D. Ediger, J. Chem. Phys. **146**, 203317 (2017).
[19]S. Mirigian and K. S. Schweizer, J. Chem. Phys. **143**, 244705 (2015).
[20]A. Bondi and D. J. Simkin, J. Chem. Phys. **25**, 1073 (1956).
[21]J. S. Chickos and W. E. Acree, J. Phys. Chem. Ref. Data **32**, 519 (2003).
[22]J. S. Chickos and D. G. Hesse, J. Org. Chem. **54**, 5250 (1989).
[23]R. Wang, C. Pellerin, and O. Lebel, J. Mater. Chem. **19**, 2747 (2009).
[24]M. K. Mapes, S. F. Swallen, and M. D. Ediger, J. Phys. Chem. B **110**, 507 (2006).
[25]S. F. Swallen and M. D. Ediger, Soft Matter **7**, 10339 (2011).
[26]S. F. Swallen, K. Traynor, R. J. McMahon, and M. D. Ediger, J. Phys. Chem. B **113**, 4600 (2009).
[27]O. Urakawa, S. F. Swallen, M. D. Ediger, and E. D. von Meerwall, Macromolecules **37**, 1558 (2004).
[28]M. Naoki and S. Koeda, J. Phys. Chem. **93**, 948 (1989).
[29]L. Zhu, J. Jona, K. Nagapudi, and T. Wu, Pharm. Res. **27**, 1558 (2010).
[30]D. J. Plazek and J. H. Magill, J. Chem. Phys. **45**, 3038 (1966).
[31]S. L. Simon, J. W. Sobieski, and D. J. Plazek, Polymer **42**, 2555 (2001).
[32]Z. Yang, Y. Fujii, F. K. Lee, C.-H. Lam, and O. K. C. Tsui, Science **328**, 1676 (2010).
[33]Y. Chai, T. Salez, J. D. McGraw, M. Benzaquen, K. Dalnoki-Veress, E. Raphael, and J. A. Forrest, Science **343**, 994 (2014).
[34]A. Forster, J. Hempenstall, I. Tucker, and T. Rades, Drug Dev. Ind. Pharm. **27**, 549 (2001).
[35]M. Yoshioka, B. C. Hancock, and G. Zografi, J. Pharm. Sci. **83**, 1700 (1994).
[36]Y. Chen, M. Zhu, A. Laventure, O. Lebel, M. D. Ediger, and L. Yu, J. Phys. Chem. B **121**, 7221 (2017).
[37]A. Nakheli, A. Elijazouli, M. Elmorabit, E. Ballouki, J. Formazero, and J. Huck, Condens. Matter **11**, 7977 (1999).
[38]B. Fábián, M. V Senćanski, I. N. Cvijetić, P. Jedlovszky, and G. Horvai, J. Phys. Chem. C **120**, 8578 (2016).
[39]R. Malshe, M. D. Ediger, L. Yu, and J. J. de Pablo, J. Chem. Phys. **134**, 194704 (2011).
[40]A. Haji-Akbari and P. G. Debenedetti, J. Chem. Phys. **141**, 024506 (2014).
[41]C. T. Powell, H. Xi, Y. Sun, E. Gunn, Y. Chen, M. D. Ediger, and L. Yu, J. Phys. Chem. B **119**, 10124 (2015).
[42]K. Six, G. Verreck, J. Peeters, M. Brewster, and G. V. D. Mooter, J. Pharm. Sci. **93**, 124 (2004).
[43]P. Espeau, R. Céolin, J.-L. Tamarit, M.-C. Perrin, J.-P. Gauchi, and F. Leveiller, J. Pharm. Sci. **94**, 524 (2005).
[44]N. S. Trasi, J. A. Baird, U. S. Kestur, and L. S. Taylor, J. Phys. Chem. B **118**, 9974 (2014).
[45]E. M. Gunn, I. A. Guzei, and L. Yu, Cryst. Growth Des. **11**, 3979 (2011).
[46]H. Konno and L. S. Taylor, J. Pharm. Sci. **95**, 2692 (2006).
[47]U. S. Kestur and L. S. Taylor, Cryst. Growth Des. **13**, 4349 (2013).
[48]J. A. Baird, B. V. Eebenbrugh, and L. S. Taylor, J. Pharm. Sci. **99**, 3787 (2010).
[49]A. K. Coker, "Appendix C: Physical properties of liquids and gases," in *Ludwig's Applied Process Design for Chemical and Petrochemical Plants*, 4th ed. (Gulf Professional Publishing, 2011), pp. 827–862.
[50]"Physical constants of organic compounds," in *CRC Handbook of Chemistry and Physics*, 2012–2013, edited by W. M. Haynes (CRC Press, Boca Raton, FL, 2012).
[51]W. V. Steele, R. D. Chirico, A. B. Cowell, S. E. Kinpmeyer, and A. Nguyen, J. Chem. Eng. Data **47**, 667 (2002).
[52]A. Laventure, A. Gujral, O. Lebel, C. Pellerin, and M. D. Ediger, J. Phys. Chem. B **121**, 2350 (2017).
[53]R. L. Leheny, N. Menon, S. R. Nagel, D. L. Price, K. Suzuya, and P. Thiyagarajan, J. Chem. Phys. **105**, 7783 (1996).
[54]S. K. Nayak, R. Sathishkumar, and T. N. G. Row, CrystEngComm **12**, 3112 (2010).
[55]BASF, "2-Ethylhexanol," Technical Leaflet M 2211 e, November 1999, available at https://www.solvents.basf.com/portal/load/fid245412/Technical/520Spec/520-/5202/520Ethylhexanol_BPC.pdf.